Mariusz Felczak,
*Gilbert De Mey,
Bogusław Więcek,
**Marina Michalak

Institute of Electronics,
Lodz University of Technology,
ul. Wolczańska 211-215, 90-924 Łódź, Poland
E-mail: felczak@p.lodz.pl

*Department of Electronics
and Information Systems
University of Ghent
Sint Pietersnieuwstraat 41, 9000 Ghent, Belgium

**Department of Material and Commodity Sciences
and Textile Metrology,
Lodz University of Technology,
ul. Wólczańska 211-215, 90-924 Łódź, Poland

Lateral and Perpendicular Thermal Conductivity Measurement on Textile Double Layers

Abstract
In this paper, the temperature distribution on a double layered fleece textile was measured experimentally with infrared thermography. A theoretical model based on the thin plate theory was to interpret the results measured. A two dimensional simulation of the same problem was carried out as well. By fitting the experimental data with the models, thermal conductivities in the lateral and perpendicular directions could be determined.

Key words: *nonwoven, thermal conductivity, heat transfer, anisotropy.*

■ Introduction

The determination of thermal characteristics of textile has become a very important matter in recent years. Knowledge of the thermal properties of textiles is not only important for the design of warm clothes, but it is also useful to understand the tactile sensing of fabrics [1 - 5]. Most investigations are limited to heat transfer by conduction in the perpendicular direction. In this paper we will focus on thermal diffusion in the lateral direction, i.e. in the plane of the fabric itself. The new, so-called smart textiles include several electronic components having characteristics depending on the ambient conditions, more specifically the temperature. An electric current flowing through an electroconductive yarn will give rise to heat generation which will be mainly spread in the lateral direction. Hence the temperature rise can be sensed by electronic components in the neighborhood of the yarn, which will influence the electrical characteristics. Moreover in the case of wearable textiles, any temperature increase will be sensed by the human body as well. The experimental setup will be used to measure the lateral thermal conductivity in combination with an analytical model to interpret the results measured. Afterwards, using a numerical model, it will be possible to determine the anisotropic thermal conductivity in a textile double layer.

The thermal properties of textile materials can also change in time due to moisture diffusion e.g. the existing methods to investigate thermal properties cannot be applied to materials with varying thermal properties. Therefore the authors present a method based on infrared thermography. The temperature distribution is then gathered in such a short time that the eventual variation in the thermal properties can be monitored by taking several thermal images one after the other.

■ Materials used

The process of heat transfer was investigated for needle punched nonwoven sets prepared by authors. From blends of 40% flax, 40% steel and 20% polyester, fleeces were produced mechanically using a carding machine. The linear densities are, respectively, 47 dtex. (flax), 9 dtex. (steel) & 1.7 dtex (polyester). The fleeces were preliminary needled and thermally pressed at a temperature of 120 °C. The polyester fibres had a low melting point so that it was possible to obtain a thin nonwoven structure. Steel fibres were inserted to increase the longitudinal thermal conductivity and are the reason for the nonwoven anisotropy. Moreover additional steel fibres were inserted in part A of the structure investigated in order to enable the probe heating (*Figure 1*).

Morphological and physical properties of the nonwoven samples were measured using the standard methods applied to textile materials. The mass per unit area was found to be $m_p = 187$ g/m^2, the density $\rho = 111$ kg/m^3 and the air permeability $Pp = 166.4$ cm^3/cm^{2}s. The nonwoven fleece structure has a thickness of about 1.7 mm.

From the nonwoven, fleece samples were fabricated. Rectangles with dimensions of 5×15 cm were cut in such a way that the fibres were parallel to the longest side. On this layer, a second one with dimensions of 5×10 cm was deposited and fixed by needling. As a result the structure shown in *Figure 1* was obtained. Thermal conductivity measurements were carried out on the double layer, with a total thickness of 3:4 mm. The single layer part was used to insert the heating elements, which were made from steel yarns, as shown in *Figure 1*.

■ Methods used

A top view of the experimental setup in shown in *Figure 2*, where a piece of fabric was mounted vertically. The first (thinnest) part AB was heated by an electric current flowing through electric conducting yarns made from steel (*Figure 1*), the aim of which was to warm up the entire fabric, including the thicker part BC, which was used for thermographic measurements. With the heat source being only connected to the thinnest part AB, it would then be possible to investigate not only the lateral heat transfer (in the x direction) but also the heat transfer between the two layers constituting the thicker part BC.

Two mirrors were also mounted vertically on both sides of the fabric [19 - 21]. The mirrors were made from aluminium in order to reflect the infrared radiation. With an thermographic camera - Cedip Titanium (USA), infrared radiation was detected from both sides, and hence the two temperature distributions $T_1(x)$ and $T_2(x)$ could be measured simultaneously
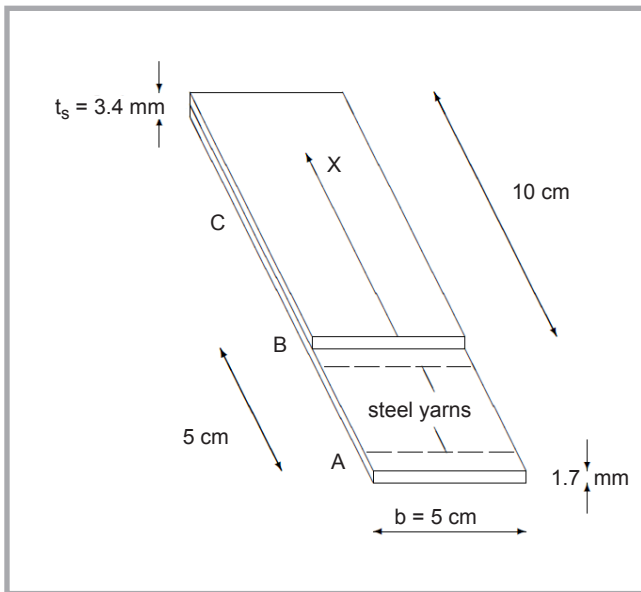
Figure 1. Isometric view of the structure investigated. Steel yarns are used for heating.
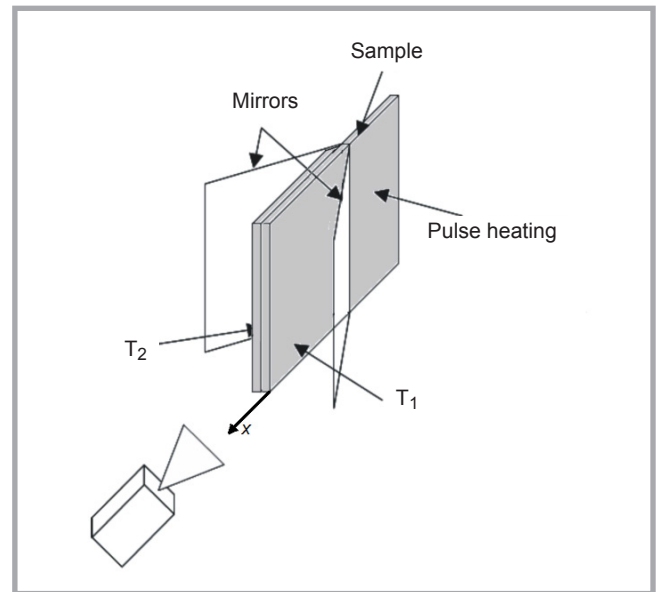

Figure 2. Top view of the experimental setup with the thermographic camera. The two mirrors allow temperature recording on both sides simultaneously [19].

[6]. Point B, where the thickness changes, was chosen as the origin to display all experimental results (x = 0). The Cedip Titanium IR camera is a QWIP (Quantum Well Infrared Photodetector) camera with an integrated Stirling cooler, which means that the camera does not have a shutter, which is used in uncooled microbolometer IR cameras. The shutter usually gets disturbed during IR measurement. The microbolometer camera could be used if a new shutterless method of thermal drift compensation was taken up [7]. The Cedip Titanium has a pixel resolution of 640 × 512/14 bits, temperature measurement accuracy of ±1 °C or ±1%, and a waveband of 3 - 5 μm. Using thermography with Fourier analysis, interesting results could also be obtained [6]. Using these methods, defects and nonuniformities in the nonwovens could also be investigated.

Experimental results are shown in *Figure 3*. Instead of $T_1(x)$ and $T_2(x)$, the sum $T_1(x) + T_2(x)$ and difference $T_1(x) - T_2(x)$ are shown. Both curves are, roughly speaking, exponential decaying functions. The spreading of lateral heat (in the x-direction) extends up to a few millimeters. At the origin x = 0 it was found that $T_1(0) = 30$ °C or 8 °C above the ambient (22 °C), whereas $T_2(0) = 27$ °C or 5 °C above the ambient. In order to prove the repeatability, a few measurements in the same conditions were made, one of which was taken for analysis.

In the paper two analyses were conducted. Theoretical analytical calculations were done using the simple thin sheet thermal model, which is one-dimensional (*Figure 1* and *Figure 4.a*), whereas the numerical model in ANSYS is two-dimensional (*Figure 4.b*). Thermal conductivity is calculated for the x and y direction. The numerical model solves Kirchoff-Fourier equations for the x and y direction. Thermal conductivity is anisotropic, thus we calculate k_x and k_y.

■ Theoretical analysis

In the theoretical analysis, we will use the thin sheet thermal model for each layer. Consequently our model will be one dimensional. Each layer has a thickness t_s, thermal conductivity k and height b. A top view is shown in *Figure 4*. The two sides exposed to ambient air are cooled convectively, expressed by heat transfer
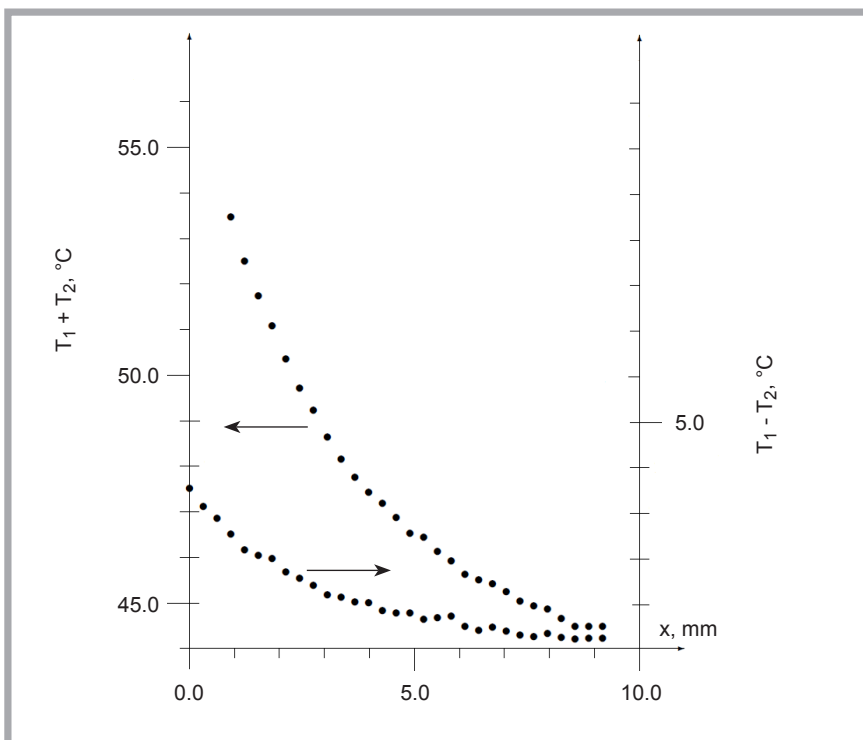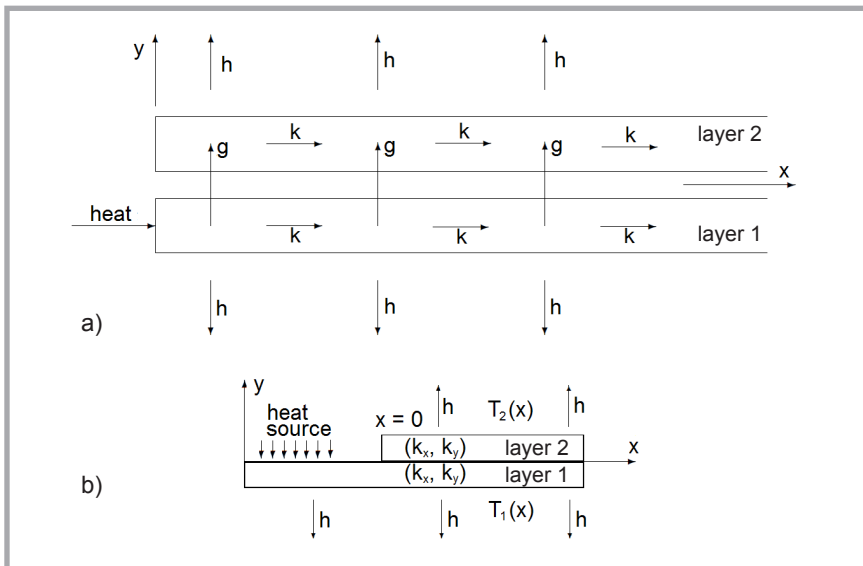

Figure 3. Experimentally measured temperature distributions. The sum and difference of the temperatures are displayed to allow easier interpretation.

Figure 4. a) Top view of mathematical model, b) view of numerical model – ANSYS.

coefficient h. Heat transfer between the two layers is expressed by conductance g in W/m²·K. If there was a third interface layer of thickness t'_s and thermal conductivity k_0 in the y direction, one would have $g = k'/t'_s$. As outlined in the foregoing section, heat is only supplied to layer 1. The other layer can only be heated through the interface, which is described in the model by conductance g. Nevertheless it is practically impossible that the second layer will not be heated directly from the heat source. Hence it will be assumed that fraction α will be supplied to layer 2 directly.

According to the thin plate theory, the differential equations for T_1 and T_2 are [8]:

$$kt_s\frac{d^2T_1}{dx^2} - hT_1 - g(T_1 - T_2) = 0 \quad (1)$$

$$kt_s\frac{d^2T_2}{dx^2} - hT_2 - g(T_2 - T_1) = 0 \quad (2)$$

where T_1 and T_2 are now temperature rises above ambient.

To solve **Equations 1** and **2**, boundary conditions are needed. First the equations will be replaced by their symmetric components. Later on the boundary conditions will be provided. It should be noted here that the boundary conditions are not strictly needed to interpret the measurements and we only need the slope of the temperature curves, as will

be explained further on. Adding and subtracting (1) and (2) yields:

$$kt_s\frac{d^2(T_1+T_2)}{dx^2} - h(T_1+T_2) = 0 \quad (3)$$

$$kt_s\frac{d^2(T_1-T_2)}{dx^2} +$$

$$- (h+2g)(T_1-T_2) = 0 \quad (4)$$

or equivalently:

$$\frac{d^2(T_1+T_2)}{dx^2} - \frac{T_1+T_2}{L_S^2} = 0 \quad (5)$$

$$\frac{d^2(T_1-T_2)}{dx^2} - \frac{T_1-T_2}{L_D^2} = 0 \quad (6)$$

where the characteristic lengths are given by:

$$L_S = \sqrt{\frac{kt_s}{h}} \qquad L_D = \sqrt{\frac{kt_s}{h+2g}} \quad (7)$$

The general solutions of (5) and (6) are:

$$T_1(x) + T_2(x) =$$

$$= (T_1(0) + T_2(0))e^{-x/L_S} \quad (8)$$

$$T_1(x) - T_2(x) =$$

$$= (T_1(0) - T_2(0))e^{-x/L_D} \quad (9)$$

In order to verify these theoretical results, the same data have been plotted on a semi logarithmic scale, as shown in **Figure 5**. The ambient temperature (22 °C) was subtracted from the experimental values because the model only provides us with temperatures increases above the ambient. Both curves can be
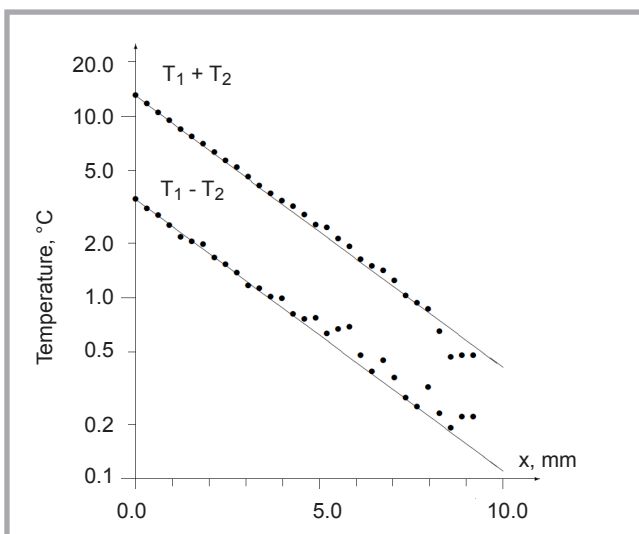

Figure 5. Experimentally measured temperature distributions (semi-logarithmic scale). The sum and difference of the temperatures.
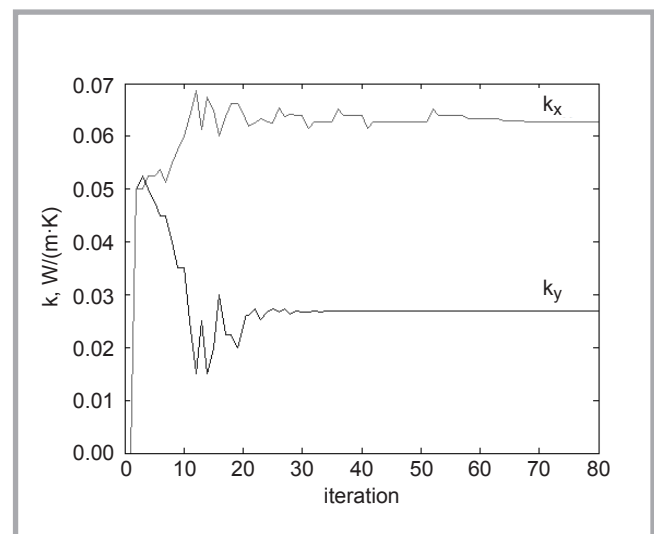

Figure 6. Lateral and perpendicular thermal conductivity k_x and k_y as a function of the iteration number.

fitted very well to straight lines despite measurement uncertainties. This proves that both curves can be represented well by exponential functions (8) and (9). It is also clear from **Figure 5** that both curves have almost the same slope, which means that both characteristic lengths L_S and L_D are equal. Consequently the value of g should be much smaller than the heat transfer coefficient h due to (7). In other words, thermal insulation between the two textile layers is quite high.

Two parallel trendlines have been drawn in **Figure 5**, corresponding to characteristic length $L_S = L_D = 2.9$ mm. As the experiments were carried out under natural convection cooling conditions, one can assume heat transfer coefficient $h = 8$ W/m²·K. Taking radiation into account, one has to add $h_r = 6$ W/m²·K, which gives rise to a total heat transfer coefficient of $h = 14$ W/m²·K. From (7) we can find the thermal conductivity of the textile layer:

$$k = \frac{hL_S^2}{t_s} = 0.0688 \; W/mK \quad (10)$$

where, thickness $t_s = 1.7$ mm was used.

The camera has an accuracy of around 1 °C. As a consequence, the measurements turn out to be not so accurate for distances $x > 5$ mm, as can be clearly seen in **Figures 3 & 5**.

In order to solve the differential equations, one needs to take into account the boundary conditions at x = 0. Assuming that a fraction α of the power supplied P is fed into layer 2 directly, the major part $(1 - \alpha)P$ is fed into layer 1:

$$-kt_sb\left(\frac{dT_1}{dx}\right)_{x=0} = (1-\alpha)P \quad (11)$$

$$-kt_sb\left(\frac{dT_2}{dx}\right)_{x=0} = \alpha P \quad (12)$$

where b is the height of the textile sample. After adding and subtracting (11) and (12), one gets:

$$-kt_sb\left(\frac{d(T_1+T_2)}{dx}\right)_{x=0} = P \quad (13)$$

$$-kt_sb\left(\frac{d(T_1-T_2)}{dx}\right)_{x=0} = (1-2\alpha)P \quad (14)$$

Filling in boundary conditions (13) and (14) in solutions (8) and (9), one obtains:

$$T_1(0) + T_2(0) = \frac{PL_S}{kt_sb} = \frac{P}{b\sqrt{kt_sh}} \quad (15)$$

$$T_1(0) - T_2(0) = \frac{PL_D}{kt_sb} =$$

$$= \frac{P(1-2\alpha)}{b\sqrt{kt_s(h+2g)}} \quad (16)$$

Taking into account that $L_S \approx L_D$, one obtains the following from (15) and (16):

$$\frac{T_1(0) - T_2(0)}{T_1(0) + T_2(0)} = 1 - 2\alpha \quad (17)$$

Experimentally we found that $T_1(0) + T_2(0) = 13$ °C and $T_1(0) - T_2(0) = 3.5$ °C, so that $\alpha = 0.37$.

■ Numerical simulation

For numerical simulation, the same geometry shown in **Figures 1 & 4** was used to carry out a two dimensional thermal analysis. Instead of considering two separate layers like layer 1 and layer 2 in **Figures 1 & 4**, a uniform material with anisotropic thermal conductivity was considered. The thermal conductivities are now k_x in the x direction and k_y in the y-direction. Anisotropy has been reported in several articles about textile materials. Anisotropy has been found in relation to mechanical [9 - 15], optical [16] and electrostatic properties [17]. Also electroconductive screen printed layers deposited on textile substrates were found to have anisotropic electric conductivities [18]. It was proved that the anisotropy was due to the structure of the textile itself and not to the conducting ink screen printed on it. Hence it is quite reasonable to accept anisotropic behaviour for the thermal conductivity.

Thermal simulations were carried out using the ANSYS software package. The program delivers two temperature distributions $T_1(x)$ and $T_2(x)$ on both sides of the nonwoven structure. This simple heat transfer problem is used to find the solution of the inversed heat transfer problem. The simple heat transfer problem receives the boundary conditions (thermal conductivity, density etc.) and outputs the temperature distribution.

The inverse heat transfer problem as the input values receives the temperature distribution and some of the boundary conditions or material parameters [22].

Depending on the inverse heat transfer problem solution method, using the temperature measured for one or more parameters can be determined. In the paper, it is thermal conductivity.

In this study, the inverse heat transfer problem was solved using the simple heat transfer model and optimisation programme created in Matlab® software. For optimisation, the algorithm golden cut method was used. The root mean square of temperatures (experimental and simulated) is minimised.

For the first simulation, arbitrary values for k_x and k_y were inputted to the optimisation program. The resulting temperature distributions are introduced automatically form the ANSYS® thermal solver to the main optimisation program. Then they are compared with the experimental values (root mean square error is calculated). In each iteration of the optimisation, new values of thermal conductivity are introduced to ANSYS®. Using the optimisation programme, it was possible to determine the thermal conductivity.

The iterations were repeated till sufficient convergence was obtained. **Figure 6** shows the values of k_x and k_y as a function of the number of iterations. A nice convergence is observed towards values $k_x = 0.0628$ W/m·K and $k_y = 0.0268$ W/m·K, clearly showing the anisotropic behaviour. During the ANSYS simulation, heat transfer coefficient $h = 8$ W/m²·K was used and also heat transfer by radiation, which corresponds to total heat transfer coefficient $h = 14$ W/m²·K, the same value as in the theoretical section. It should be mentioned here that the simulation result for k_x agrees very well with the value $k = 0.0688$ W/m·K obtained from the theoretical model outlined in the previous section. It should also be noted that the value $k_y = 0.0268$ W/m·K is very low, comparable with the thermal conductivity of most insulating materials. In the theoretical section, the conductivity in the y direction was found to be almost zero, which is due to the fact that a simpler model was used, whereas the ANSYS simulation was a fully two dimensional analysis.

Conclusion

Thermographic measurements were carried out on a piece of textile made from a double layered fleece material. One of the layers was heated, whereas the other one could only be heated through conduction from the first one. A theoretical model was set up for this textile structure and the results compared with the experimental data. It was found that the perpendicular conduction was almost non-existant. The lateral thermal conductivity was found to be $k = 0.0688$ W/m·K. With ANSYS software a two dimensional simulation was carried out as well. The lateral and perpendicular thermal conductivities were found to be $k_x = 0.0628$ W/m·K and $k_y = 0.0268$ W/m·K, respectively. The conclusion is that the simple analytical model is suited to determine the lateral thermal conductivity. To measure both conductivities, a more detailed two dimensional model is required. It should be noted that the temperature drops at a length constant at around 3 mm. Hence only a small area is suited for measurements, which is not a problem if thermography is used.

References

1. Ciesielska-Wróbel IL, Van Langenhove L. Fingertip skin models for analysis of the haptic perception of textiles. *J. Biomedical Science and Engineering* 2014; 7: 1-6.
2. Ciesielska-Wróbel IL, Van Langenhove L. The hand of textiles – definitions, achievements, perspectives. *Textile Research Journal* 2012; 82: 1457-1468.
3. Mazzuchetti R, Demichelis MB, Songia F, Rombaldoni. Objective Measurement of Tactile Sensitivity Related to a Feeling of softness and Warmth. *Fibers & Textiles in Eastern Europe* 2008; 16, 4(69): 67-71.
4. Takako Inoue, Akira Nakayama, Masako Niwa. Relationship between the warm/cool feeling of fabric and the subjective evaluation of the quality of ladies' knitted fabrics. *International Journal of Clothing Science and Technology* 2010; 22, 1: 7-15.
5. Yoneda M, Kawabata S. Analysis of Transient Heat Conduction in Textiles and Its Applications. Part II. *Journal of Textile Machinery Society of Japan* 1983; 31: 73-81.
6. Świątczak T, Tomczyk M, Więcek B, Pawlak R, Olbrycht R. Defect detection in wire welded joints using thermography investigations. *Materials Science and Engineering* 2012; 1239-1242.
7. Olbrycht R, Więcek B, De Mey G. *Thermal drift compensation method for microbolometer thermal cameras*. Applied Optics, 2012.
8. Cengel Y. *Heat transfer a practical approach*. 2nd Edition, New York, McGraw Hill 2003, pp.785-842.
9. Sun-Pui Roger Ng, Winnie Yu. Bilinear approximation of anisotropic stress strain properties of woven fabrics. *Research Journal of Textile and Apparel* 2005; 9: 50-56.
10. Suh MW, Gnay M, Jasper WP. Prediction of surface uniformity in woven fabrics through 2-D anisotropic measures. Part I: Definition and theoretical model. *Journal of the Textile Institute* 2007; 98: 109-116.
11. Klvaityle R. and Masteikaite V. Anisotropy of woven fabric deformation after stretching. *Fibres & Textiles in Eastern Europe* 2008; 16: 52-56.
12. Zouari R, Amar SB, Dogui A. Experimental and numerical analyses of fabric off axes tensile test. *Journal of Textile Institute* 2008; 101: 58-68.
13. Sidabraite V, Masteikaite V. Effect of woven fabric anisotropy on drape behaviour. *Materials Science* 2003; 9: 111-115.
14. Frontczak-Wasiak I, Snycerski M, Stępien Z, Suszek H. Measuring method of ultidirectional force distribution in a woven fabric. *Fibres & Textiles in Eastern Europe* 2004, vol.12, pp. 48-51.
15. Zheng JM. Takatera M. Inui S. and Shimizu Y. Measuring technology of the anisotropic tensile properties of woven fabrics. *Textile Research Journal* 2008; 78(12): 1116-1123.
16. Yazaki Y, Takatera M, Yoshio Shimizu M. Anistropic light transmission properties of plain woven fabrics. *Sen'I Gakkaishi* 2004; 60: 41-46.
17. Azoulay J. Anisotropy in electrical properties of fabrics containing new conductive fibers. In: *IEEE Transactions on Electrical Insulation* 1988; 23: 383-386.
18. Kazani I, De Mey G, Banaszczyk J, Schwarz A, Hertleer C, Van Langenhove L. Van Der Pauw method for measuring resistivities of anisotropic layers deposited on textile substrates. *Textile Research Journal* 2011. doi: 10.1177/0040517511416280.
19. Michalak M., Felczak M., Wiecek B. Evaluation of the Thermal Parameters of Textile Materials Using the Thermographic Method. *Fibres & Textiles In Eastern Europe* 2009; 17, 3(74): 84-89.
20. Michalak M, Więcek B. Estimating the thermal properties of flat products by a new non-contact method. *Fibres & Textiles in Eastern Europe* 2008; 16, 4(69): 72-77.
21. Michalak M. Application of the non-contact thermal method for estimation of the thermal parameters of flat materials. *Fibres & Textiles in Eastern Europe* 2010; 18, 6(83): 76-79.
22. Ozisik NM, Orlande HRB. *Inverse Heat Transfer: Fundamentals and Applications* 2000; Hemisphere Pub.